Expedited Articles

Structure-Based Discovery of Small Molecule Inhibitors Targeted to Protein Tyrosine Phosphatase 1B

Mauro Sarmiento,[†] Li Wu,[‡] Yen-Fang Keng,[‡] Li Song,[§] Zhaowen Luo,[§] Ziwei Huang,[§] Guo-Zhang Wu,[||] Adam K. Yuan,[||] and Zhong-Yin Zhang*,[†,‡]

Departments of Molecular Pharmacology and Biochemistry, The Albert Einstein College of Medicine of Yeshiva University, 1300 Morris Park Avenue, Bronx, New York 10461, Kimmel Cancer Institute, Jefferson Medical College, Thomas Jefferson University, Philadelphia, Pennsylvania 19107, and Tyger Scientific Inc., 11 Deer Park Drive, Monmouth Junction, New Jersey 08852

Received June 25, 1999

Protein tyrosine phosphatases (PTPases) are involved in the control of tyrosine phosphorylation levels in the cell and are believed to be crucial for the regulation of a multitude of cellular functions. A detailed understanding of the role played by PTPases in various signaling pathways has not yet been achieved, and potent and selective PTPase inhibitors are essential in the quest to determine the functionality of individual PTPases. Using the DOCK methodology, we have carried out a structure-based, computer-assisted search of an available chemical database in order to identify low molecular weight, nonpeptidic PTP1B inhibitors. We have identified several organic molecules that not only possess inhibitory activity against PTP1B but which also display significant selectivity for PTP1B. This indicates that although structural features important for pTyr recognition are conserved among different PTPases, it is possible to generate selective inhibitors targeted primarily to the catalytic site. Kinetic analysis and molecular modeling experiments suggest that the PTP1B active site possesses significant plasticity such that substituted and extended aromatic systems can be accommodated. The newly identified molecules provide a molecular framework upon which therapeutically useful compounds can ultimately be based, and systematic optimization of these lead compounds is likely to further enhance their potency and selectivity.

Introduction

Protein tyrosine phosphatases (PTPases) make up a diverse family of enzymes which is important for controlling the status of tyrosine phosphorylation and regulation of numerous cellular functions.[1,2] The PTPase family is presently comprised of approximately 100 enzymes which are either receptor-like or cytoplasmic. The hallmark for this family of enzymes is the PTPase signature motif, (H/V)**C**X_5**R**(S/T), housed within the catalytic domain.[3] Genetic and biochemical evidence indicate that PTPases are involved in a number of disease processes.[3] Unfortunately, a detailed understanding of the role played by PTPases in various signaling pathways has been hampered by the absence of PTPase-specific inhibitors.

Our interest in PTPase inhibitors is focused on PTP1B, a prototypic intracellular PTPase that is expressed in a wide variety of human tissues.[4] PTP1B has been implicated as a negative regulator of insulin receptor signaling.[5−9] Clinical studies have found a correlation between insulin resistance states and levels of PTP1B expression in muscle and adipose tissues, suggesting that PTP1B may play a role in the insulin resistance associated with diabetes and obesity.[10−12] A recent pivotal PTP1B knockout study revealed that mice lacking functional PTP1B exhibit increased sensitivity toward insulin and are resistant to obesity.[13] These results, taken together, establish a direct role for PTP1B in down regulating the insulin functions. Highly selective PTP1B inhibitors would be of decided utility in helping to identify PTP1B in vivo substrates and in examining the specific regulatory role that PTP1B plays in insulin signaling. Additionally, specific inhibition of PTP1B may be therapeutically beneficial in the treatment of Type II diabetes mellitus, insulin resistance, and obesity.

Most of the PTP1B inhibitors which have been previously described are peptide-based, containing negatively charged sulfate or phosphonic acid derivatives. These compounds are inefficient in crossing cell membranes and are unstable in vivo. Thus, it was our goal to identify small organic compounds which exhibit potent and selective inhibitory profiles against PTP1B. Systematically docking compounds from chemical databases to molecular targets of known structure has become a

* To whom correspondence should be addressed: Department of Molecular Pharmacology, Albert Einstein College of Medicine, 1300 Morris Park Avenue, Bronx, NY 10461. Tel: 718-430-4288. Fax: 718-430-8922. E-mail: zyzhang@aecom.yu.edu.
[†] Department of Biochemistry, The Albert Einstein College of Medicine of Yeshiva University.
[‡] Department of Molecular Pharmacology, The Albert Einstein College of Medicine of Yeshiva University.
[§] Thomas Jefferson University.
[||] Tyger Scientific Inc.

10.1021/jm990329z CCC: $19.00
Published on Web 12/28/1999

powerful tool in the discovery of enzyme inhibitors,[14−18] novel enzyme substrates,[19] ligands targeted to an RNA double helix,[20] and nonpeptidic compounds which block protein−protein interactions.[21,22] Since three-dimensional structures of PTP1B in complex with various substrates are available,[23,24] we describe here a structure-based computer screening approach for the discovery of low molecular weight nonpeptidic PTP1B inhibitors. Using the DOCK methodology,[25] we have identified several organic molecules that not only possess high affinity for PTP1B but also display significant selectivity against LAR, PTPα, and the dual specificity phosphatase VHR.

Results and Discussion

DOCK Analysis. Progress in defining the physiological roles of PTPases has been hampered by the lack of potent and selective inhibitors. The DOCK program is designed to identify novel compounds complementary to the ligand binding site of an enzyme or receptor of known 3D structure.[26] In this study, we seek to identify small molecule inhibitors targeted to PTP1B by using the DOCK approach. The crystal structure employed in this computer-based screening is PTP1B bound with pTyr at 1.8 Å resolution,[24] the highest resolution PTP1B structure to date. We focused primarily on the active site pocket encompassing the pTyr binding site and its immediate surroundings. The DOCK algorithm[21] was used to screen about 150 000 compounds in the Available Chemicals Directory (Molecular Design Limited Information Systems, San Leandro, CA) for compounds displaying good geometric and electrostatic complementarity to the PTP1B active site. The putative interactions between the top scoring compounds, which included 1000 from the distance-based and 1000 from the force field-based screen, and PTP1B were examined individually in order to select a subset of compounds for biological testing. The following criteria were employed for compound selection: (1) chemical diversity; (2) modes of interaction with the enzyme active site; (3) overall fit and how well the compound complemented the shape of the pocket without protruding into solvent; and (4) solubility, chemical stability, commercial availability, and cost. From the original 2000 compounds identified by DOCK, 25 were purchased for testing as PTPase inhibitors. Of these 25, 17 were chosen based on distance screens and 8 based on force field screens.

Kinetic Characterization of the Compounds Selected from the DOCK Screen. The ability of the 25 compounds selected from the DOCK screening to inhibit the PTP1B-catalyzed hydrolysis of *p*-nitrophenyl phosphate (*p*NPP) was assessed at pH 7 and 30 °C (for details, see Experimental Section). Seven out of the 25 compounds examined in the enzyme assay exhibited measurable inhibition of PTP1B at 100 μM concentration. The structures of these seven compounds are shown in Figure 1. To further characterize the interactions between these compounds and PTP1B, the inhibition constant and the mode of inhibition were determined by steady-state kinetic analysis of the PTPase with 8 different substrate concentrations and 3 different inhibitor concentrations. The results are summarized in Table 1. As shown in Figure 2, the effect of compound

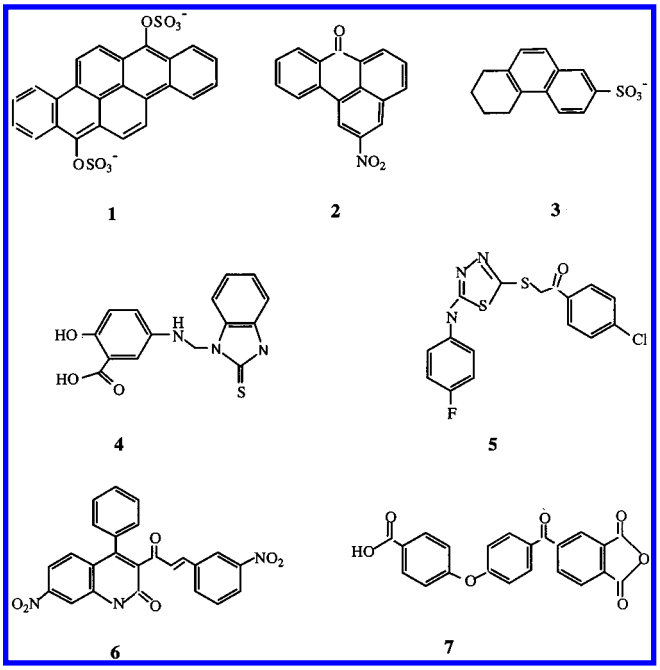

Figure 1. Structures of PTP1B inhibitors identified by DOCK: **1**, dibenz[*b*,*i*]pyrene-1,6-disulfate; **2**, 2-nitrobenzanthrone; **3**, 5,6,7,8-tetrahydro-2-phenanthrenesulfonic; **4**, 5-(2,3-dihydro-2-thioxo-1-benzimidazolylmethylamino)salicylic acid; **5**, 1-(4-chlorophenyl)-2-[(5-(4-fluoroanilino)-1,3.4-thiadiazol-2-yl)thio]ethane-1-one; **6**, 7-nitro-3-(3-(3-nitro-phenyl)-acryloyl)-4-phenyl-1*H*-quinolon-2-one; **7**, 4-(4-(1,3-dioxo-1,3-dihydro-isobenzofuran-5-carbonyl)-phenoxy)benzoic acid.

Table 1. Inhibition Constants (μM) of Compounds **1**−**7** as Inhibitors of PTP1B, PTPα, LAR, and VHR

compd[a]	PTP1B	PTPα	LAR	VHR
1	$K_{is} = 39 \pm 8$	>100[b]	>100[b]	>100[b]
2	$K_{is} = 21 \pm 5$	>100[b]	$K_{is} = 68 \pm 20$	>100[b]
	$K_{ii} = 34 \pm 6$		$K_{ii} = 57 \pm 10$	
3	$K_{is} = 240 \pm 50$	$K_{is} = 410 \pm 120$	>1000[c]	>1000[c]
4	$K_{is} = 61 \pm 3$	$K_{is} = 180 \pm 50$	>100[b]	>100[b]
5	$K_{is} = 110 \pm 34$	$K_{is} = 57 \pm 5$	$K_{is} = 53 \pm 8$	>100[b]
	$K_{ii} = 131 \pm 18$		$K_{ii} = 92 \pm 11$	
6	$K_{is} = 54 \pm 6$	>100[b]	>100[b]	>100[b]
7	$K_{is} = 510 \pm 50$	>1000[c]	>1000[c]	>1000[c]

[a] The compound numbering corresponds to that given in Figure 1. [b] No inhibition detected at 100 μM concentration. [c] No inhibition detected at 1000 μM concentration.

4 on the PTP1B-catalyzed *p*NPP hydrolysis displayed the characteristic intersecting line pattern for competitive inhibition. Similarly, compounds **1**, **3**, **6**, and **7** also displayed competitive inhibition of PTP1B with respect to the substrate *p*NPP. Interestingly, compounds **2** and **5** displayed mixed inhibition patterns (data not shown), suggesting that these two compounds bind to both free enzyme and the enzyme−substrate complex.

It is known that conserved amino acids from prokaryotic to eukaryotic PTPases[27] are located in and around the active site.[28−32] Some of these amino acid residues maintain the active site's shape, while others are involved in binding pTyr and/or catalysis. As shown in the crystal structures of PTP1B/C215S complexed with pTyr,[23,24] invariant nonpolar residues in the PTPase catalytic domains (Tyr46, Val49, Phe182, and Gln262 in PTP1B) form the binding site for the phenyl ring of pTyr, while the phosphoryl group of pTyr is surrounded by residues corresponding to the PTPase signature motif (residues 215−222 in PTP1B). This suggests that the

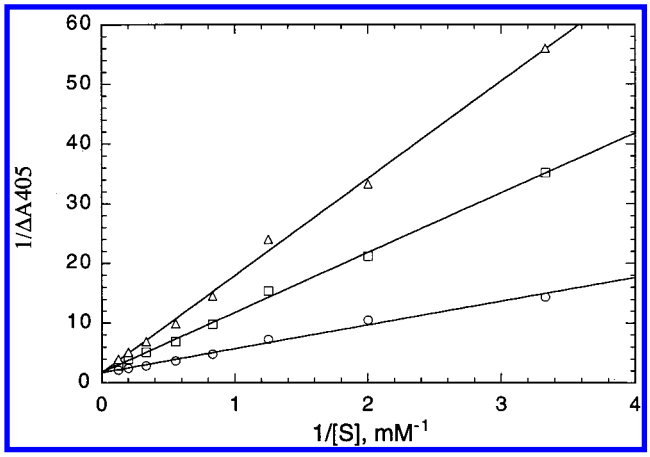

Figure 2. Effect of compound **4** on the PTP1B-catalyzed hydrolysis of *p*NPP. The experiment was performed at 30 °C, pH 7.0. Compound **4** concentrations were 0 (○), 100 (□), and 200 μM (△), respectively.

mechanism for pTyr recognition is similar among all PTPases. However, it is important to note that the active sites are not identical among the different PTPases. Since our docking analysis was based on the active site structure of PTP1B, it is of interest to determine whether the compounds identified display any selectivity against other PTPases.

We therefore examined the effect of the compounds which inhibited PTP1B on the receptor-like PTPases, LAR and PTPα, both of which have also been implicated as negative regulatory agents in the insulin-mediated signal transduction pathways.[3] The effect of these compounds on the human dual specificity phosphatase VHR, the best characterized member of this subfamily of phosphatases, was also investigated. As shown in Table 1, none of the compounds showed significant inhibition of the VHR-catalyzed reaction at the concentrations indicated. This inability to inhibit VHR is not surprising, given the known dissimilarities in primary and tertiary structures between the tyrosine-specific PTPases[28−32] and the dual specificity phosphatases.[33,34] Compound **5** inhibited PTP1B, LAR, and PTPα equally well. The inhibitory efficacy of **2** was 2-fold higher for PTP1B than for LAR, whereas it exhibited no inhibition against PTPα. Compound **3** and **4** inhibited PTP1B and PTPα with a 2- and 3-fold selectivity, respectively, in favor of PTP1B. In contrast, neither **3** nor **4** were particularly effective inhibitors of LAR. Remarkably, compounds such as **1**, **6**, and **7** did not appreciably inhibit LAR or PTPα at the highest attainable concentrations and exhibited a strong preference for PTP1B relative to the other tyrosine-specific PTPases implicated in the insulin-driven signaling pathways. These results demonstrate that it should be feasible to develop potent, selective, active site-directed inhibitors for individual members of the PTPase family of enzymes.

Structural Basis for PTP1B Inhibition by Compound 1. The identification of compounds **1** and **3** as potential PTP1B inhibitors from the DOCK screening was not surprising, since aryl sulfate esters/sulfonic acids are structural analogues of aryl phosphate esters/phosphonic acids. Considering the structural similarity of aryl sulfate/sulfonate moieties to pTyr and the DOCK-predicated modes of binding for **1** and **3**, in which the aryl sulfate/sulfonate moieties approximate the interactions between pTyr and the active site of PTP1B, the competitive inhibition pattern seen for **1** and **3** was expected. It has been previously shown that sulfotyrosyl-containing peptides are not hydrolyzed by PTPases but rather act as competitive inhibitors of the PTPase-catalyzed reactions.[35,36] We have recently demonstrated that suramin, a molecule containing multiple aryl sulfonates, is also a competitive, reversible PTPase inhibitor.[37] Thus, the fact that **1** and **3** were identified from the active site-targeted DOCK and inhibited PTP1B competitively validates the docking approach.

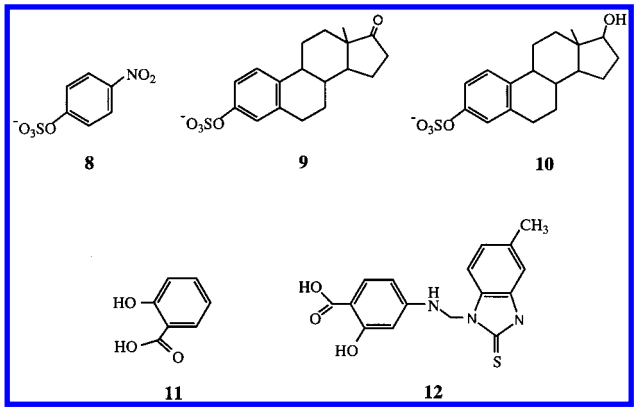

Figure 3. Structures of compounds with similar structural features to **1** and **4**: **8**, *p*-nitrophenyl sulfate; **9**, estrone-3-sulfate; **10**, estradiol-3-sulfate; **11**, salicylic acid; **12**, 4-*N*-(2-mercapto-5-methylbenzimidazolyl)methylaminosalicylic acid.

Table 2. Inhibition Constants (μM) of Compounds **8**−**12** as Inhibitors of PTP1B

compd[a]	PTP1B
8	$K_{is} = 10000 \pm 1000$
9	$K_{is} = 2100 \pm 100$
10	no inhibition at 1 mM
11	$K_{is} = 19400 \pm 630$
12	$K_{is} = 750 \pm 90$

[a] The compound numbering corresponds to that given in Figure 3.

The observed potency and selectivity of compound **1** toward PTP1B is striking. Although compound **1** contains a phenyl sulfate element, the overall size of the molecule is much bulkier than pTyr. To gain further insight about the structural features of **1** responsible for the high affinity binding, we tested the ability of *p*-nitrophenyl sulfate (**8**), estrone-3-sulfate (**9**), and estradiol-3-sulfate (**10**) (Figure 3) to inhibit PTP1B. As shown in Table 2, *p*-nitrophenyl sulfate and estrone-3-sulfate inhibited PTP1B activity competitively, with a K_{is} value of 10 and 2.1 mM, respectively. Estradiol-3-sulfate did not inhibit PTP1B at 1 mM concentration. Because the affinity of *p*-nitrophenyl sulfate for PTP1B is 250-fold lower than that of compound **1**, the extended aromatic ring system, in addition to the aryl sulfate motif, must be important for high affinity binding. Indeed, it has been previously shown that difluorophosphonomethyl phenyl compounds are poor inhibitors of PTP1B, whereas the corresponding naphthyl derivatives exhibit enhanced affinities.[38] The X-ray crystal structure of PTP1B in complex with [1,1-diflouro-1-(2-naphthalenyl)-methyl] phosphonic acid[39] revealed extensive hydrophobic interactions between PTP1B and the naphthyl ring, which is not available to the single phenyl ring. The inability of estrone-3-sulfate and estradiol-3-sulfate to inhibit PTP1B effectively also

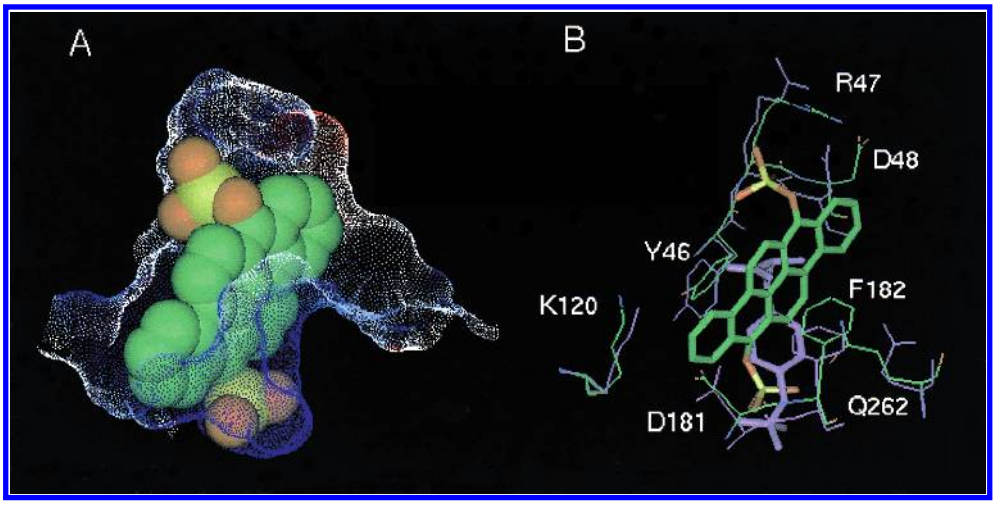

Figure 4. (A) Connolly surface of the active site of the simulated PTP1B·**1** complex. Surface is colored by the electrostatic potential (basic/blue, acidic/red) calculated using the Insight II (95.0) module DelPhi. Compound **1** is rendered in CPK form. (B) Backbone superimposition of the simulated PTP1B·**1** complex (by atom type, i.e., C, in green, N, in blue, S, in yellow, and O, in red) and the crystal structure of PTP1B·pTyr (in purple).[24] The backbones and side chains of those residues undergoing the greatest movement in response to **1** binding are depicted.

suggests that a planar ring system is preferred by PTP1B. Thus, a great deal of plasticity must exist in the PTP1B active site so that it can accommodate molecules significantly larger than pTyr and bind bulky polyaromatic systems.

To rationalize the observed binding affinity of compound **1** to PTP1B, we performed dynamic simulations and energy minimizations on the PTP1B·**1** complex determined by DOCK. As can be seen from the dynamic-simulated and energy-minimized structure (Figure 4A), compound **1** is effectively buried within the active site of PTP1B, clearly demonstrating the hydrophobic potential and flexibility of the pocket. In this structure, the planar ring system of **1** is able to form extensive interactions with PTP1B: aromatic−aromatic interactions with Tyr46 and Phe182, van der Waals contacts with the aliphatic side chains of Arg47, Asp48, Val49, Glu115, Lys120, Asp181, and Ile219, and polar interactions with the side chain of Gln262. In addition, the sulfate group of **1** facing the active site forms hydrogen bonds with the backbone amides of Ser216, Ala217, Gly218, and Gly220 and the side chain of Arg221 (Figure 5). Compared to the original orientation determined by DOCK, Arg47 has moved approximately 4.0 Å toward **1** in the energy-minimized structure of the PTP1B·**1** complex. Consequently, a long hydrogen bond (3.8 Å) between one of the oxygens of the sulfate distal from the pTyr site and the guanidinium group of Arg47 is now possible (Figures 4B and 5). According to the structure,[24] the guanidinium group of Arg47 does not interact directly with pTyr (or *p*NPP). Indeed, mutations at residue 47 did not lead to any alteration in the rate of PTP1B-catalyzed *p*NPP hydrolysis.[40] If Arg47 plays a role in binding compound **1** by interacting directly with the sulfate group, then abrogation of this interaction should lead to a decrease in binding affinity. Indeed, compound **1** inhibited PTP1B/R47E with a K_{is} value of 276 μM, a 7-fold decrease in affinity relative to wild-type PTP1B. This result validates the observed interaction between Arg47 and **1** and confirms the importance of Arg47 in inhibitor binding.

A comparison between the putative modes of interaction of **1** with PTP1B and that of pTyr with PTP1B

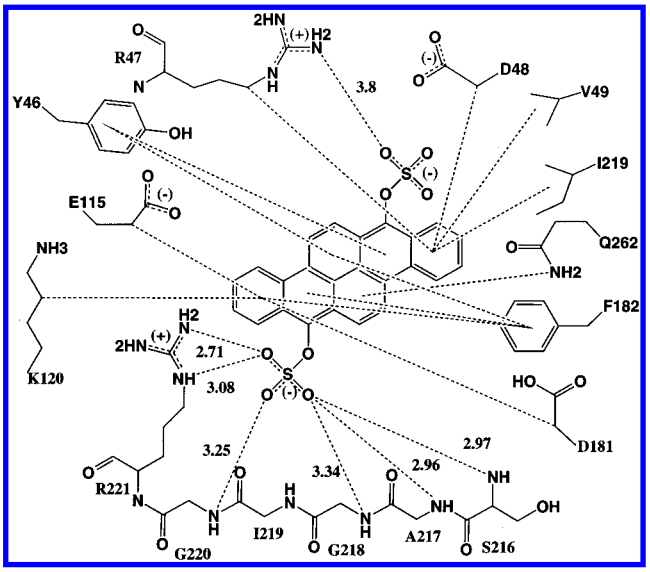

Figure 5. Schematic representation of the interactions between the simulated structure of PTP1B and compound **1**.

(Figure 4B) suggests that although both **1** and pTyr are capable of binding to the catalytic site of PTP1B, major differences between the two complexes exist. For example, the binding of the phosphoryl group in pTyr to PTP1B is dominated by hydrogen-bonding interactions between the phosphate oxygens and the amide nitrogens of the phosphate-binding loop and the guanidinium group of the invariant Arg221.[23,24] Compound **1** maintains some of these hydrogen bonds between its sulfate oxygens and the amides of Ser216, Ala217, Gly218, and Gly220 and the side chain of Arg221 (Figure 5). But, it appears that the interaction between the active site directed sulfate and the phosphate-binding loop is somewhat weaker than that between the phosphate group of pTyr and PTP1B. Compound **1** instead attempts to maximize hydrophobic interactions between its extended ring system and those residues surrounding the active site pocket of PTP1B. Consequently, the bulky ring system of **1** has adopted a unique binding mode that results from numerous structural readjustments in PTP1B (Figure 4B). Not surprisingly, the observed

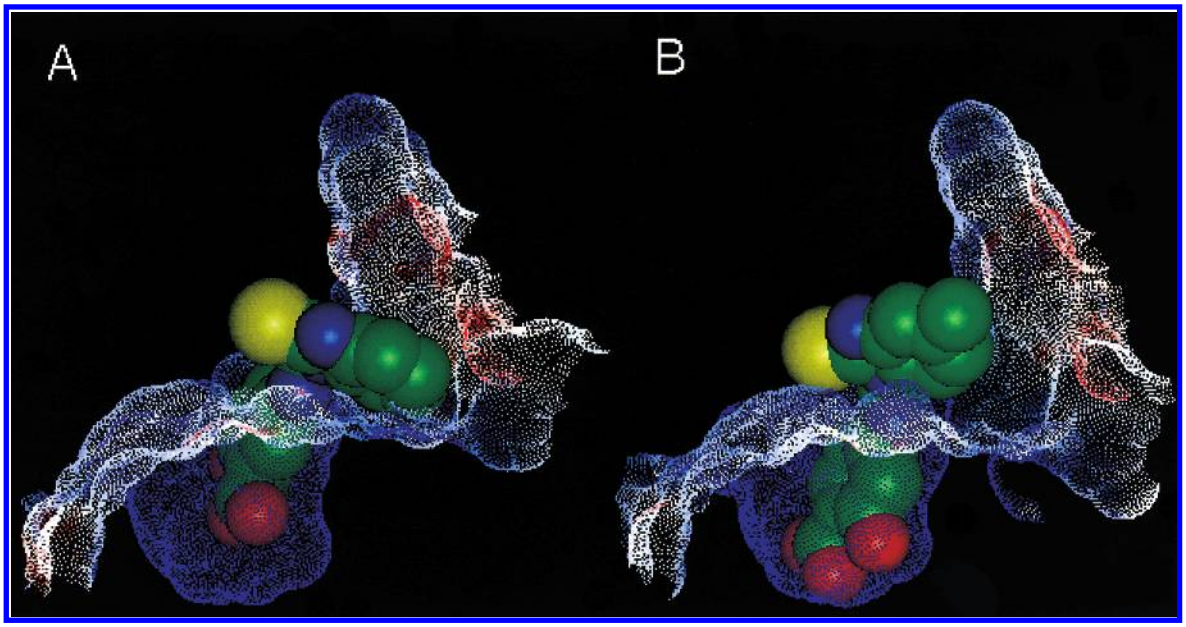

Figure 6. Connolly surface of the active site of the simulated (A) PTP1B·**4** and (B) PTP1B·**12** complexes. Surface is colored by the electrostatic potential (basic/blue and acidic/red) calculated using the Insight II (95.0) module DelPhi. Compounds **4** and **12** are both rendered in CPK forms, in which carbon is shown in green, oxygen in red, sulfur in yellow, and nitrogen in blue.

structural perturbations are largely felt by the side chains of those residues which define the depth of the active site pocket, as the position of the peptide backbone in the PTP1B·**1** complex undergoes only slight changes in comparison to the PTP1B·pTyr structure. In particular, the side chain orientations of Tyr46, Asp48, Lys120, Asp181, Phe182, and Gln262 shift in order to optimize interactions with the planar ring system of **1**. Some of these interactions are also observed between pTyr and PTP1B in the PTP1B·pTyr complex. For example, Tyr46 maintains $\pi-\pi$ interactions with **1**, Phe182 remains in a perpendicular orientation relative to **1**, and the polar side chain of Gln262 still faces the ring system of **1** for maximum interaction (Figure 4B). However, additional contacts are formed which are not possible with a single phenyl ring. Most notable is the new van der Waals contacts between **1** and the aliphatic side chains of Asp48, Glu115, Asp181, and Lys120. These interactions are not possible between pTyr and PTP1B and may help to offset weaker electrostatic interactions between PTP1B and **1** and to enhance the overall binding of **1** versus pTyr.

Structural Basis for PTP1B Inhibition by Compound 4. We were excited by the finding that compound **4** acted as a high affinity competitive inhibitor of PTP1B. The binding orientation, as suggested by DOCK, shows that the salicylic acid moiety in **4** approximates the binding mode of pTyr in PTP1B and, consequently, many of the interactions seen between the phosphate moiety and the phosphate-binding loop in the PTP1B·pTyr structure are conserved between PTP1B and **4**. This suggests that salicylic acid may serve as a new non-phosphorus-containing pTyr mimic, utilizing carboxylic acid and hydroxyl groups to provide functionality normally afforded by the phosphoryl group in pTyr. It is worth noting that the benzoic acid moiety of compound **7** is also predicted by DOCK to occupy the catalytic site of PTP1B. The observed competitive inhibition pattern of **7** corroborates this proposed orientation and suggests that benzoic acid can also serve as a non-phosphorus-containing pTyr mimic.

To test if the mode of interaction between PTP1B and **4** is as suggested by DOCK, we assayed whether salicylic acid (**11**) itself would inhibit PTP1B. Indeed, salicylic acid is a competitive inhibitor of PTP1B with an inhibition constant of 19.4 mM (Table 2). This is consistent with the notion that the salicylic acid moiety in **4** occupies the pTyr binding site. However, like pTyr and all pTyr surrogates (see below), salicylic acid does not possess a high affinity for PTP1B. Since many of the interactions between pTyr and PTP1B are predicted by DOCK to be conserved between PTP1B and the salicylic acid moiety of **4**, additional interactions must occur which contribute to the 320-fold enhancement in the observed binding of **4** versus salicylic acid. These additional interactions likely involve extensive hydrophobic contacts between the 2-thioxo-1-benzimidazolyl fused ring of **4** and surface residues of PTP1B.

To further substantiate the mode of interaction between PTP1B and **4** suggested by DOCK, we also prepared compound **12**. Compound **12** is a structural analogue of **4** in which the positions of the hydroxyl and the carboxyl groups in the salicylic acid moiety are switched and an extra methyl group is appended to the benzimidazolyl ring (Figure 3). It was of interest to determine whether introduction of these changes into **4** would affect its affinity to PTP1B. We found that although compound **12** still inhibited PTP1B competitively, its potency was reduced by more than 12-fold as compared with compound **4** (Table 2). Thus, the modifications made to **4** still allow **12** to bind to the PTP1B active site, but additional contacts unique to **4** have been lost.

To better understand the manner by which compounds **4** and **12** interact with PTP1B, molecular modeling was performed. The simulated complexes of compounds **4** and **12** with PTP1B revealed major differences in binding modes (Figure 6). It appears that

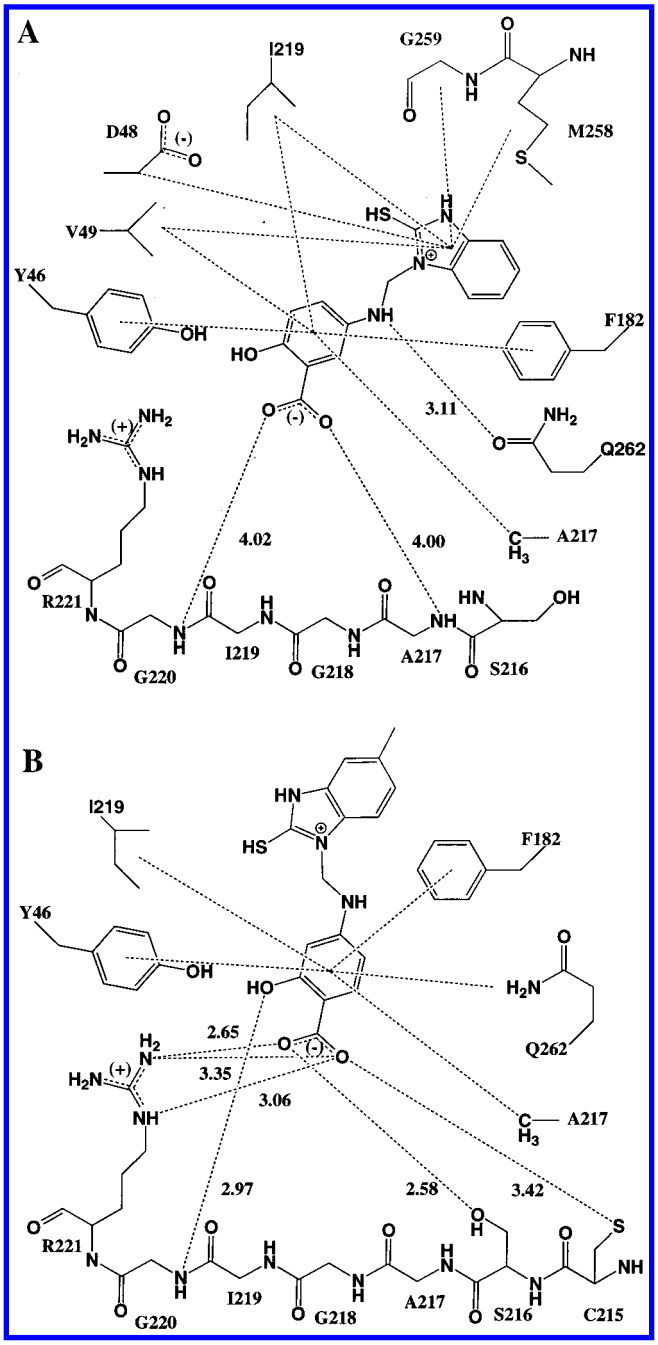

Figure 7. Schematic representation of the interactions between the simulated structure of PTP1B and compound **4** (A) and those of PTP1B and compound **12** (B).

compound **12** attempts to maximize the hydrogen-bonding potential of its carboxylic and hydroxyl groups in a manner similar to pTyr. Thus, the carboxylate and hydroxyl of **12** are able to form hydrogen bonds with the backbone amide of Gly220 and the side chains of Cys215, Ser216, and Arg221 (Figure 7B). In addition to these electrostatic interactions, the phenyl ring of the salicylic acid moiety is in an orientation similar to that of pTyr. Consequently, the phenyl ring of **12** forms analogous contacts with the aromatic side chains of Tyr46 and Phe182, the aliphatic side chains of Ala217 and Ile219, and with the polar side chain of Gln262. This attempt to maximize the interactions between the salicylic acid moiety and PTP1B forces the fused 2-mercapto-5-methylbenzimidazolyl ring of compound **12** to move away from the enzyme surface (Figure 6B). Consequently, this movement prohibits additional hydrophobic interactions with PTP1B and can be charged with the deleterious effect on the reduced inhibition of PTP1B by compound **12**. On the other hand, compound **4** is oriented within the pTyr pocket which maximizes both electrostatic and hydrophobic interactions with PTP1B (Figure 6A). Hydrogen bonds exist between the hydroxyl and carboxylic groups of compound **4** and the phosphate-binding loop, albeit less extensive than those seen with **12**. These electrostatic interactions occur specifically with backbone amides of Ala217 and Gly220 (Figure 7A). The phenyl ring maintains hydrophobic interactions with residues Tyr46, Val49, Phe182, Ala217, Ile219, and Gln262. In addition, extensive hydrophobic interactions between the fused benzimidazolyl ring of compound **4** and a proximal hydrophobic pocket formed by Val49, Ile219, Met258, and Gln262 are also observed. Interestingly, this hydrophobic pocket of PTP1B is also responsible for the binding of the Leu side chain at the P+1 position of the peptide substrate DADEpYL-NH_2[23] and is capable of binding a second aryl phosphate.[24] The abundant hydrophobic interactions with the fused benzimidazolyl ring likely account for compound **4**'s superior inhibitory effect over compound **12** (Figure 6). Collectively, these results suggest that the orientation of **4** determined by DOCK is likely correct and that further structure-based systematic modification of the lead structure will yield PTP1B-selective inhibitors with much enhanced affinity. In this regard, we note that additional flexibility introduced to the linker region of compound **12** may generate a better inhibitor which allows the simultaneous capitalization of interactions with both the salicylic acid moiety and the benzimidazolyl ring.

PTP1B Inhibition by Compound 6. It is interesting to note that the 3-nitrophenyl acryloyl moiety of **6** was predicted by DOCK to occupy the pTyr binding site in PTP1B. Molecular modeling based on this initial starting structure also revealed potential interactions between the enzyme and the inhibitor. In this complex, the nitro group in the 3-nitrophenyl acryloyl moiety is able to form hydrogen bonds with backbone amides of the phosphate-binding loop and the side chain of Arg221, and the phenyl ring can interact with the side chains of Tyr46, Phe182, Ala217, Ile217, and Gln262. Additionally, the nitro group in the quinolon moiety is positioned in proximity to Arg47, possibly forming hydrogen bonds with the basic side chain. Indeed, compound **6** inhibited PTP1B competitively with a K_{is} value of 54 μM, whereas it did not inhibit either LAR or PTPα, phosphatases which lack a basic residue at this position. To assess the validity to this proposed interaction, we again employed the PTP1B/R47E mutant. Not surprisingly, compound **6** inhibited PTP1B/R47E competitively with a K_{is} value of 124 μM, 2.3-fold higher than wild-type PTP1B, supporting a direct interaction between the guanidinium group of Arg47 and the nitro group in the quinolon moiety in **6**. Thus, like compound **4**, compound **6** represents another structure upon which systematic structure−activity studies may lead to potent and selective low molecular weight PTP1B inhibitors. Compounds **2** and **5** displayed mixed inhibition against PTP1B and were relatively nonspecific. Further kinetic and structural investigation is

required to understand the structural and chemical basis for their inhibition.

Effective pTyr Surrogates. It has been shown that the phosphoryl group in pTyr[41,42] and amino acids flanking the pTyr[43,44] both contribute to high affinity substrate binding by PTPases. Thus, one approach toward the design of potent and selective PTPase inhibitors relies on the incorporation of a nonhydrolyzable pTyr mimetics into a specific, optimal peptide template. The most commonly used phosphorus-based pTyr analogues are phosphonomethyl phenylalanine (Pmp)[44,45] and phosphonodifluoromethyl phenylalanine (F_2Pmp).[46,47] However, there is a concern that the dianionic nature of the phosphonate group may compromise its ability to cross cell membranes.

The doubly negative charge is not absolutely required for PTPase binding because we have shown that both the monoanion and the dianion forms of the phosphonate bind PTP1B with equal efficiency.[48] Furthermore, there exist monoanionic sulfotyrosine and several nonphosphorus-based carboxylate-containing pTyr surrogates, such as *O*-malonyltyrosine (OMT),[49] fluoro-*O*-malonyl tyrosine (FOMT),[50] cinnamic acid,[51] and 3-carboxy-4-(*O*-carboxymethyl) tyrosine.[52] Like pTyr, none of these pTyr mimetics alone exhibit high affinity toward PTPases. However, when attached to an appropriate peptide template, the pTyr surrogate-containing peptides are effective PTPase inhibitors.

We have shown here that salicylic acid, benzoic acid, and nitrophenyl moiety can also act as pTyr analogues. In addition, our results suggest that sulfate and appropriately positioned carboxyl and hydroxyl groups can replace or mimic the pTyr phosphate group and its interactions with the PTPase signature motif. We have also shown that potent and selective nonpeptidyl low molecular weight inhibitors of PTP1B can be obtained when a properly functionalized phosphate surrogate is attached to an appropriate aromatic framework, which effectively occupies the pTyr pocket and interacts with the immediate surroundings beyond the catalytic site, thereby enhancing both inhibitor affinity and specificity.

Conclusion

Through docking analysis, we have identified several novel, low molecular weight PTP1B inhibitors. Some of the inhibitors are relatively specific to PTP1B, indicating that although structural features important for pTyr recognition are conserved among different PTPases, it is possible to generate selective inhibitors targeted primarily to the catalytic site and its immediate surroundings. The average sequence homology among PTPase catalytic domains is 40%, a value sufficiently low to suggest that the individual members of the PTPase family may recognize distinct specificity determinants. The potent inhibition exhibited by the compounds identified illustrates the power of the DOCK approach for the discovery of a diverse array of low molecular weight compounds which have not been shown previously to be PTPase inhibitors. In combination with molecular modeling studies, our results suggest that the pTyr-binding site (the active site) of PTP1B possesses significant plasticity such that substituted and extended aromatic systems can be accommodated. Also, our results suggest that additional binding regions proximal to the active site are important in inhibitor development. Through DOCK and subsequent optimization, potent—yet highly selective—PTPase inhibitors can be developed which should not only be useful in dissecting the precise roles played by specific PTPases in signal transduction, but which may ultimately provide a molecular basis upon which therapeutically useful agents can be designed.

Experimental Section

Materials. All chemicals were obtained from commercial suppliers and used without further purification. *p*-Nitrophenyl phosphate (*p*NPP) was from Fluka Co. Estrone-3-sulfate, estradiol-3-sulfate, and salicylic acid were obtained from Sigma. Selected compounds from DOCK screening were purchased from the Sigma-Aldrich Library of Rare Chemicals (SALOR), Aldrich, Sigma, or Maybridge.

Synthesis of 4-*N*-(2-Mercapto-5-methylbenzimidazolyl)-methylamino salicylic Acid.[53] A mixture of 2-mercapto-5-methylbenzimidazole (1.6 g, 0.01 mol) and 50 mL of ethanol was heated to a clear solution at 60 °C before addition of formaldehyde (37% water solution, 1.1 g, 0.013 mol). 4-Aminosalicylic acid (1.5 g, 0.01 mol) in 30 mL of ethanol solution was added into the reaction mixture dropwise, and the reaction was incubated at 60 °C for 1 h. The resulting reaction mixture was concentrated to 30 mL of solution and cooled in a freezer overnight. The resulting white precipitate was collected and washed with ethanol. The final product was recrystallized in ethanol and characterized by proton NMR.

Computer Screening. DOCK 3.5,[54] a structure-based search program, was utilized for the identification of specific small molecule inhibitors of PTP1B. The DOCK program[25,55−57] is specifically designed for the identification of putative ligands which are complementary to a targeted surface area. In brief, DOCK first generates a negative image of the ligand binding site with a set of overlapping spheres whose centers become the potential locations for ligand atoms. To rank each potential ligand, a precalculated contact-scoring grid, based on distances between potential ligand and target area atoms, and a force field-scoring grid, based on molecular mechanics interaction energies consisting of van der Waals and electrostatic components, were generated.[57] The resulting output file for each screening, based on distance or force field grids, contains the highest scoring compounds ranked in order of their scores. These high scoring compounds can then be subjected to further examination and purchased for biological evaluation. The Available Chemicals Directory (ACD 95.2, Molecular Design Limited, San Leando, CA) was used as the compound database to be screened for potential ligands.

The high resolution structure of PTP1B/C215S in complex with pTyr[24] was used for the DOCK study. Ser215 was mutated back to the wild type Cys by using the Residue/Replace command of the Biopolymer module of Insight II (97.0). The thiolate form of Cys215 was employed in the docking experiments. The solvent-accessible surface of the pTyr-binding site and its immediate area was described by clusters of overlapping spheres. The specific sphere cluster utilized was a manually edited cluster comprised of 38 individual spheres, which satisfactorily covered the target area. About 150,000 compounds in the ACD were screened. On average, 400 orientations (nmatch) were sampled for each molecule docked. In addition, rigid body minimization was used at maximum 500 steps (with convergence = 0.2 Å). No chemical labeling was used in the matching calculation. The top 1000 scoring compounds were selected from each distance- and force field-based DOCK screen. From these lists, an effort was made to choose compounds that were chemically diverse and which appeared to interact with the enzyme active site in different modes. Compound selection was based on several criteria. Most importantly, overall fit was determined by how

well the compound complemented the shape of the pocket without protruding into solvent. Additionally, chosen compounds were soluble, unreactive, commercially available, and of low cost. Selection was performed on a R4400 SGI workstation using the computer-graphics program INSIGHT II (Biosym Technologies, San Diego, CA). Three sequential screens were performed in which the above criteria were employed. From the original 2000 compounds selected, 25 were purchased for testing against the PTPases. Of these 25 compounds, 17 were chosen based on distance and 8 from force field screens.

Molecular Modeling. All molecular dynamics simulations and minimizations were performed using the Discover_3 module of Insight II (95.0) on a Silicon Graphics Indigo^2 R4400 workstation. The starting structure utilized was the PTP1B bound with pTyr,[24] including crystal waters, in which Ser215 was mutated back to a cysteine residue. Compound **4** was docked into the active site in the orientation determined by DOCK. Compound **12** was placed into the active site by superimposing its phenyl ring onto the equivalent phenyl ring of compound **4**. Movable regions included all residues and crystal waters within 10 Å of the docked compound. An 18 Å sphere of water was placed and centered around each compound. The CVFF force field was employed, and the cell-multiple method for nonbonded interactions was utilized. All simulations followed a stepwise protocol of molecular dynamics and minimizations, consisting of the following: (1) 1000 steps of conjugate gradient minimization using the Polak-Ribiere method; (2) 5 ps of molecular dynamics simulations at 598 K; (3) 10 ps of molecular dynamics simulations at 498 K; (4) 15 ps of molecular dynamics simulations at 398 K; (5) 20 ps of molecular dynamics simulations at 348 K; (6) 80 ps of molecular dynamics simulations at 298 K. As determined by the individual plots of total energy and temperature versus time, equilibrium was achieved within 1000 fs at the 298 K stage of molecular dynamics. During this period, data collection occurred every 500 steps, and the 153 steps gathered at equilibrium were used to determine the average conformation. All figures reflect this average complex, and the electrostatic potential of the active-site surface was calculated using the default parameters of the DelPhi module of Insight II (95.0).

Recombinant PTP1B, LAR, PTPα, and VHR. Human PTP1B was expressed and purified as previously described.[58] The R47E mutant form of PTP1B was generated using the Muta-Gene in vitro mutagenesis kit from Bio-Rad and purified as described.[40] The pGEX plasmid containing the coding sequence for both of the PTPase domains of human PTPα was a generous gift from Dr. Frank Jirik of the University of British Columbia. The recombinant glutathione S-transferase (GST) fusion protein was purified, and the intracellular fragment of PTPα containing both of the PTPase domains was cleaved off the fusion protein as described.[59] Recombinant LAR containing both PTPase domains was purified as described.[60] Recombinant VHR dual specificity phosphatase was purified to homogeneity according to a published procedure.[61]

Inhibition Study. All compounds were dissolved in 100% dimethyl sulfoxide (DMSO). All reactions, including controls, were performed at a final concentration of 10% DMSO. The initial rate of PTPase-catalyzed hydrolysis of *p*NPP was measured as described.[62] The selected compounds were first evaluated for their ability to inhibit the PTPase reaction at 100 μM concentration at 30 °C in a reaction volume (0.2 mL) with 2 mM of *p*NPP. The assay buffer was 50 mM 3,3-dimethylglutarate, 10% DMSO, pH 7.0, with ion strength of 0.15 M adjusted by sodium chloride. The reaction was initiated by addition of the enzyme and quenched after 2−3 min by addition of 1 mL of 1 N NaOH. The amount of *p*-nitrophenol produced was determined from the A_{405} using a molar extinction coefficient of 18 000 M^{-1} cm^{-1}. The nonenzymatic hydrolysis of the substrate was corrected by measuring controls of substrate without the addition of the enzyme. The effect of 10% DMSO on normal enzyme activity was assayed and determined to be negligible. Those compounds which demonstrated any inhibition were further characterized. Inhibition constants for the PTPase inhibitors were determined for PTP1B, LAR, PTPα, and VHR in the following manner. The initial rate at eight different *p*NPP concentrations (0.2 K_m to 5 K_m) was measured at three different fixed inhibitor concentrations.[63] The inhibition constant was obtained, and the inhibition pattern evaluated using a direct curve-fitting program KINETASYST (IntelliKinetics, State College, PA). The following equations were used to fit the initial rate data of the enzyme-catalyzed reaction:

For competitive inhibition,

$$v = V_{max}S/[K_m(1 + I/K_{is}) + S] \quad (1)$$

For mixed inhibition,

$$v = V_{max}S/[K_m(1 + I/K_{is}) + S(1 + I/K_{ii})] \quad (2)$$

For uncompetitive inhibition,

$$v = V_{max}S/[K_m + S(1 + I/K_{ii})] \quad (3)$$

The following nomenclature is used:[64] v, initial velocity; V_{max}, maximum velovity; S, substrate concentration; K_m, apparent Michaelis constant; I, inhibitor concentration; K_{is} and K_{ii}, slope and intercept inhibition constants, respectively.

Acknowledgment. This work was supported in part by a Research Award from the American Diabetes Association and by a Pilot Research Project Award from the Cancer Center of the Albert Einstein College of Medicine (Z.-Y. Z.). Z.-Y. Z. is a Sinsheimer Scholar and an Irma T. Hirschl Career Scientist. M.S. was supported by National Institutes of Health Grant 5T32 GM 07491-21. We thank Daniel McCain and Monica E. Hamburgh for helpful comments on this manuscript and for Daniel McCain's assistance in the preparation of Figures 5 and 7.

References

(1) Hunter, T. Protein Kinases and Phosphatases: the Yin and Yang of Protein Phosphorylation and Signaling. *Cell* **1995**, *80*, 225−236.
(2) Tonks, N. K.; Neel, B. G. From Form to Function: Signaling by Protein Tyrosine Phosphatases. *Cell* **1996**, *87*, 365−368.
(3) Zhang, Z.-Y. Protein-Tyrosine Phosphatases: Biological Function, Structural Characteristics, and Mechanism of Catalysis. *CRC Crit. Rev. Biochem. Mol. Biol.* **1998**, *33*, 1−52.
(4) Chernoff, J.; Schievella, A. R.; Jost, C. A.; Erikson, R. L.; Neel, B. G. Cloning of a cDNA for a Major Human Protein-Tyrosine-Phosphatase. *Proc. Natl. Acad. Sci. U.S.A.* **1990**, *87*, 2735−2739.
(5) Ahmad, F.; Li, P.-M.; Meyerovitch, J.; Goldstein, B. J. Osmotic Loading of Neutralizing Antibodies Demonstrates a Role for Protein-Tyrosine Phosphatase 1B in Negative Regulation of the Insulin Action Pathway. *J. Biol. Chem.* **1995**, *270*, 20503−20508.
(6) Kenner, K. A.; Anyanwu, E.; Olefsky, J. M.; Kusari, J. Protein-Tyrosine Phosphatase 1B Is a Negative Regulator of Insulin- and Insulin-like Growth Factor I−Stimulated Signaling. *J. Biol. Chem.* **1996**, *271*, 19810−19816.
(7) Kole, H. K.; Garant, M. J.; Kole, S.; Bernier, M. A Peptide-Based Protein-Tyrosine Phosphatase Inhibitor Specifically Enhances Insulin Receptor Function in Intact Cells. *J. Biol. Chem.* **1996**, *271*, 14302−14307.
(8) Bandyopadhyay, D.; Kusari, A.; Kenner, K. A.; Liu, F.; Chernoff, J.; Gustafson, T. A.; Kusari, J. Protein-Tyrosine Phosphatase 1B Complexes with the Insulin Receptor in vivo and Is Tyrosine-Phosphorylated in the Presence of Insulin. *J. Biol. Chem.* **1997**, *272*, 1639−1645.
(9) Chen, H.; Wertheimer, S. J.; Lin, C. H.; Amrein, K. E.; Burn, P.; Quon, M. J. Protein-Tyrosine Phosphatases PTP1B and Syp Are Modulators of Insulin-Stimulated Translocation of GLUT4 in Transfected Rat Adipose Cells. *J. Biol. Chem.* **1997**, *272*, 8026−8031.
(10) Kusari, J.; Kenner, K. A.; Suh, K.-I.; Hill, D. E.; Henry, R. R. Skeletal Muscle Protein Tyrosine Phosphatase Activity and Tyrosine Phosphatase 1B Protein Content Are Associated with Insulin Action and Resistance. *J. Clin. Invest.* **1994**, *93*, 1156−1162.
(11) Ahmad, F.; Azevedo, J. L.; Cortright, R.; Dohm, G. L.; Goldstein, B. J. Alterations in Skeletal Muscle Protein-Tyrosine Phosphatase Activity and Expression in Insulin-Resistant Human Obesity and Diabetes. *J. Clin. Invest.* **1997**, *100*, 449−458.

(12) Ahmad, F.; Considine, R. V.; Bauer, T. L.; Ohannesian, J. P.; Marco, C. C.; Goldstein, B. J. Improved Sensitivity to Insulin in Obese Subjects following Weight Loss Is Accompanied by Reduced Protein-Tyrosine Phosphatases in Adipose Tissue. *Metabolism* **1997**, *46*, 1140−1145.
(13) Elchelby, M.; Payette, P.; Michaliszyn, E.; Cromlish, W.; Collins, S.; Lee Loy, A.; Normandin, D.; Cheng, A.; Himms-Hagen, J.; Chan, C.-C.; Ramachandran, C.; Gresser, M. J.; Tremblay, M. L.; Kennedy, B. P. Increased Insulin Sensitivity and Obesity Resistance in Mice Lacking the Protein Phosphatase-1B Gene. *Science* **1999**, *283*, 1544−1548.
(14) Desjarlais, R. L.; Seibel, G. L.; Kuntz, I. D.; Furth, P. S.; Alvarez, J. C.; Ortiz de Montellano, P. R.; DeCamp, D. L.; Babe, L. M.; Craik, C. S. Structure-Based Design of Nonpeptide Inhibitors Specific for the Human Immunodeficiency Virus 1 Protease. *Proc. Natl. Acad. Sci. U.S.A.* **1990**, *87*, 6644−6648.
(15) Ring, C. S.; Sun, E.; McKerrow, J. H.; Lee, G. K.; Rosenthal, P. J.; Kuntz, I. D.; Cohen, F. E. Structure-Based Inhibitor Design by Using Protein Models for the Development of Antiparasitic Agents. *Proc. Natl. Acad. Sci. U.S.A.* **1993**, *90*, 3583−3587.
(16) Shoichet, B. K.; Stroud, R. M.; Santi, D. V.; Kuntz, I. D.; Perry, K. M. Structure-Based Discovery of Inhibitors of Thymidylate Synthase. *Science* **1993**, *259*, 1445−1450.
(17) Gschwend, D. A.; Sirawaraporn, W.; Santi, D. V.; Kuntz, I. D. Specificity in Structure-Based Drug Design: Identification of a Novel, Selective Inhibitor of Pneumocystis Carinii Dihydrofolate Reductase. *Proteins: Struct., Funct., Genet.* **1997**, *29*, 59−67.
(18) Somoza, J. R.; Skillman, A. G.; Munagala, N. R.; Oshiro, M. C.; Knegtel, R. M. A.; Mpoke, S.; Fletterick, R. J.; Kuntz, I. D.; Wang, C. C. Rational Design of Novel Antimicrobials: Blocking Purine Salvage in a Parasitic Protozoan. *Biochemistry* **1998**, *37*, 5344−5348.
(19) De Voss, J. J.; Sibbesen, O.; Zhang, Z.; Ortiz de Montellano, P. R. Substrate Docking Algorithms and Predictions of the Substrate Specificity of Cytochrome $P450_{cam}$ and Its L244A Mutant. *J. Am. Chem. Soc.* **1997**, *119*, 5489−5498.
(20) Chen, Q.; Shafer, R. H.; Kuntz, I. D. Structure-Based Discovery of Ligands Targeted to the RNA Double Helix. *Biochemistry* **1997**, *36*, 11402−11407.
(21) Li, S.; Gao, J.; Satoh, T.; Friedman, T. M.; Edling, A. E.; Koch, U.; Choksi, S.; Han, X.; Korngold, R.; Huang, Z. A Computer Screening Approach to Immunoglobulin Superfamily Structures and Interactions: Discovery of Small Nonpeptidic CD4 Inhibitors as Novel Immunotherapeutics. *Proc. Natl. Acad. Sci. U.S.A.* **1997**, *94*, 73−78.
(22) Li, S.; Satoh, T.; Korngold, R.; Huang, Z. CD4 Dimerization and Oligomerization: Implications for T-cell Function and Structure-Based Drug Design. *Immunol. Today* **1998**, *19*, 455−462.
(23) Jia, Z.; Barford, D.; Flint, A. J.; Tonks, N. K. Structural Basis for Phosphotyrosine Peptide Recognition by Protein Tyrosine Phosphatase 1B. *Science* **1995**, *268*, 1754−1758.
(24) Puius, Y. A.; Zhao, Y.; Sullivan, M.; Lawrence, D. S.; Almo, S. C.; Zhang, Z.-Y. Identification of a Second Aryl Phosphate-Binding Site in Protein-Tyrosine Phosphatase 1B: A Paradigm for Inhibitor Design. *Proc. Natl. Acad. Sci. U.S.A.* **1997**, *94*, 13420−13425.
(25) Kuntz, I. D.; Meng, E. C.; Shoichet, B. K. Structure-Based Molecular Design. *Acc. Chem. Res.* **1994**, *27*, 117−123.
(26) Kuntz, I. D. Structure-Based Strategies for Drug Design and Discovery. *Science* **1992**, *257*, 1078−1082.
(27) Zhang, Z.-Y.; Wang, Y.; Dixon, J. E. Dissecting the Catalytic Mechanism of Protein-Tyrosine Phosphatases. *Proc. Natl. Acad. Sci. U.S.A.* **1994**, *91*, 1624−1627.
(28) Barford, D.; Flint, A. J.; Tonks, N. K. Crystal Structure of Human Protein Tyrosine Phosphatase 1B. *Science* **1994**, *263*, 1397−1404.
(29) Stuckey, J. A.; Schubert, H. L.; Fauman, E.; Zhang, Z.-Y.; Dixon, J. E.; Saper, M. A. Crystal Structure of Yersinia Protein Tyrosine Phosphatase at 2.5 A and the Complex with Tungstate. *Nature* **1994**, *370*, 571−575.
(30) Bilwes, A. M.; den Hertog, J.; Hunter, T.; Noel, J. P. Structural Basis for Inhibition of Receptor Protein-Tyrosine Phosphatase-Alpha by Dimerization. *Nature* **1996**, *382*, 555−559.
(31) Hoffmann, K. M. V.; Tonks, N. K.; Barford, D. The Crystal Structure of Domain 1 of Receptor Protein-Tyrosine Phosphatase mu. *J. Biol. Chem.* **1997**, *272*, 27505−27508.
(32) Hof, P.; Pluskey, S.; Dhe-Paganon, S.; Eck, M. J.; Shoelson, S. E. Crystal Structure of the Tyrosine Phosphatase SHP-2. *Cell* **1998**, *92*, 441−450.
(33) Fauman, E. B.; Cogswell, J. P.; Lovejoy, B.; Rocque, W. J.; Holmes, W.; Montana, V. G.; Piwnica-Worms, H.; Rink, M. J.; Saper, M. A. Crystal Structure of the Catalytic Domain of the Human Cell Cycle Control Phosphatase, Cdc25A. *Cell* **1998**, *93*, 617−625.
(34) Yuvaniyama, J.; Denu, J. M.; Dixon, J. E.; Saper, M. A. Crystal Structure of the Dual Specificity Protein Phosphatase VHR. *Science* **1996**, *272*, 1328−1331.
(35) Liotta, A. S.; Kole, H. K.; Fales, H. M.; Roth, J.; Bernier, M. A Synthetic Tris-Sulfotyrosyl Dodecapeptide Analogue of the Insulin Receptor 1146-Kinase Domain Inhibits Tyrosine Dephosphorylation of the Insulin Receptor in situ. *J. Biol. Chem.* **1994**, *269*, 22996−23001.
(36) Desmarais, S.; Jia, Z.; Ramachandran, C. Inhibition of Protein Tyrosine Phosphatases PTP1B and CD45 by Sulfotyrosyl Peptides. *Arch. Biochem. Biophys.* **1998**, *354*, 225−231.
(37) Zhang, Y.-L.; Keng, Y.-F.; Zhao, Y.; Wu, L.; Zhang, Z.-Y. Suramin Is an Active Site-Directed, Reversible, and Tight-Binding Inhibitor of Protein-Tyrosine Phosphatases. *J. Biol. Chem.* **1998**, *273*, 12281−12287.
(38) Kole, H. K.; Smyth, M. S.; Russ, P. L.; Burke, T. R., Jr. Phosphonate Inhibitors of Protein-Tyrosine and Serine/Threonine Phosphatases. *Biochem. J.* **1995**, *311*, 1025−1031.
(39) Burke, T. R., Jr.; Ye, B.; Yan, X.; Wang, S.; Jia, Z.; Chen, L.; Zhang, Z.-Y.; Barford, D. Small Molecule Interactions with Protein-Tyrosine Phosphatase PTP1B and Their Use in Inhibitor Design. *Biochemistry* **1996**, *35*, 15989−15996.
(40) Sarmiento, M.; Zhao, Z.; Gordon, S. J.; Zhang, Z.-Y. Molecular Basis for Substrate Specificity of Protein-tyrosine Phosphatase 1B. *J. Biol. Chem.* **1998**, *273*, 26368−26374.
(41) Zhang, Z.-Y.; Maclean, D.; Thieme-Sefler, A. M.; Roeske, R.; Dixon, J. E. A Continuous Spectrophotometric and Fluorimetric Assay for Protein Tyrosine Phosphatase Using Phosphotyrosine-Containing Peptides. *Anal. Biochem.* **1993**, *211*, 7−15.
(42) Ruzzene, M.; Donella-Deana, A.; Marin, O.; Perich, J. W.; Ruzza, P.; Borin, G.; Calderan, A.; Pinna, L. A. Specificity of T-Cell Protein Tyrosine Phosphatase toward Phosphorylated Synthetic Peptides. *Eur. J. Biochem.* **1993**, *211*, 289−295.
(43) Zhang, Z.-Y.; Thieme-Sefler, A. M.; Maclean, D.; McNamara, D. J.; Dobrusin, E. M.; Sawyer, T. K.; Dixon, J. E. Substrate Specificity of the Protein Tyrosine Phosphatases. *Proc. Natl. Acad. Sci. U.S.A.* **1993**, *90*, 4446−4450.
(44) Zhang, Z.-Y.; Maclean, D.; McNamara, D. J.; Dobrusin, E. M.; Sawyer, T. K.; Dixon, J. E. Protein Tyrosine Phosphatase Substrate Specificity: Size and Phosphotyrosine Positioning Requirements in Peptide Substrates. *Biochemistry* **1994**, *33*, 2285−2290.
(45) Chatterjee, S.; Goldstein, B. J.; Csermely, P.; Shoelson, S. E. Phosphopeptide Substrates and Phosphonopeptide Inhibitors of Protein-Tyrosine Phosphatases. In *Peptides*, (*Proceedings of the Twelfth American Peptide Symposium*); 1992; pp 553−555, Leiden, The Netherlands.
(46) Burke, T. R., Jr.; Smyth, M.; Nomizu, M.; Otaka, A.; Roller, P. P. Preparation of Flouro- and Hydroxy-4-(phosphonomethyl)-D,L-phenylalanine Suitably Protected for Solid-Phase Synthesis of Peptides Containing Hydrolytically Stable Analogues of *O*-Phosphotyrosine *J. Org. Chem.* **1993**, *58*, 1336−1340.
(47) Burke, T. R., Jr.; Kole, H. K.; Roller, P. P. Potent Inhibition of Insulin Receptor Dephosphorylation by a Hexamer Peptide Containing the Phosphotyrosyl Mimetic F_2Pmp. *Biochem. Biophys. Res. Commun.* **1994**, *204*, 129−134.
(48) Chen, L.; Wu, L.; Otaka, A.; Smyth, M. S.; Roller, P. P.; Burke, T. R., Jr.; den Hertog, J.; Zhang, Z.-Y. Why Is Phosphonodifluoromethyl Phenylalanine a More Potent Inhibitory Moiety than Phosphonomethyl Phenylalanine toward Protein Tyrosine Phosphatases? *Biochem. Biophys. Res. Commun.* **1995**, *216*, 976−984.
(49) Kole, H. K.; Akamatsu, M.; Ye, B.; Yan, X.; Barford, D.; Roller, P. P.; Burke, T. R., Jr. Protein-Tyrosine Phosphatase Inhibition by a Peptide Containing the Phosphotyrosyl Mimetic, L-O-Malonyltyrosine. *Biochem. Biophys. Res. Commun.* **1995**, *209*, 817−822.
(50) Roller, P. P.; Wu, L.; Zhang, Z.-Y.; Burke, T. R., Jr. Potent Inhibition of Protein-Tyrosine Phosphatase-1B Using the Phosphotyrosyl Mimetic Fluoro-O-Malonyl Tyrosine (FOMT). *Bioorg. Med. Chem. Lett.* **1998**, *8*, 2149−2150.
(51) Moran, E. J.; Sarshar, S.; Cargill, J. F.; Shahbaz, M. M.; Lio, A.; Mjalli, A. M. M.; Armstrong, R. W. Radio Frequency Tag Encoded Combinatorial Library Method for the Discovery of Tripeptide-Substituted Cinnamic Acid Inhibitors of the Protein Tyrosine Phosphatase PTP1B *J. Am. Chem. Soc.* **1995**, *117*, 10787−10788.
(52) Burke, T. R., Jr.; Yao, Z.-J.; Zhao, H.; Milne, G. W. A.; Wu, L.; Zhang, Z.-Y.; Voigt, J. H. Enantioselective Synthesis of Non-phosphorous-Containing Phosphotyrosyl Mimetics and Their Use in the Preparation of Tyrosine Phosphatase Inhibitory Peptides. *Tetrahedron* **1998**, *54*, 9981−9994.
(53) Ram, V. J.; Pandey, H. N. 1,3,4-Oxadiazoles. III Mannich Bases Derived from 5-(O−Hydroxyphenyl)-1,3,4-Oxadiazole-2-Thione *J. Indian Chem. Soc.* **1974**, *51*, 634−635.
(54) Gschwend, D. A.; Kuntz, I. D. Orientational Sampling and Rigid-Body Minimization in Molecular Docking Revisited: On-the-Fly Optimization and Degeneracy Removal. *J. Comput.-Aided. Mol. Des.* **1996**, *10*, 123−132.

(55) Kuntz, I. D.; Blaney, J. M.; Oatley, S. J.; Langridge, R.; Ferrin, T. E. A Geometric Approach to Macromolecule-Ligand Interactions. *J. Mol. Biol.* **1982**, *161*, 269−288.
(56) Shoichet, B. K.; Bodian, D. L.; Kuntz, I. D. Molecular Docking Using Shape Descriptors. *J. Comput. Chem.* **1992**, *13*, 380−397.
(57) Meng, E. C.; Shoichet, B. K.; Kuntz, I. D. Automated Docking with Grid-Based Energy Evaluation. *J. Comput. Chem.* **1992**, *13*, 505−524.
(58) Zhang, Y.-L.; Zhang, Z.-Y. Low-Affinity Binding Determined by Titration Calorimetry Using a High-Affinity Coupling Ligand: a Thermodynamic Study of Ligand Binding to Protein Tyrosine Phosphatase 1B. *Anal. Biochem.* **1998**, *261*, 139−148.
(59) Guan, K. L.; Dixon, J. E. Eukaryotic Proteins Expressed in *Escherichia coli*: An Improved Thrombin Cleavage and Purification Procedure of Fusion Proteins with Glutathione S-Transferase. *Anal. Biochem.* **1991**, *192*, 262−267.
(60) Pot, D. A.; Woodford, T. A.; Remboutsika, E.; Haun, R. S.; Dixon, J. E. Cloning, Bacterial Expression, Purification, and Characterization of the Cytoplasmic Domain of Rat LAR, a Receptor-Like Protein Tyrosine Phosphatase. *J. Biol. Chem.* **1991**, *266*, 19688−19696.
(61) Zhang, Z.-Y.; Wu, L.; Chen, L. Transition State and Rate-Limiting Step of the Reaction Catalyzed by the Human Dual-Specificity Phosphatase, VHR. *Biochemistry* **1995**, *34*, 16088−16096.
(62) Zhang, Z.-Y. Kinetic and Mechanistic Characterization of a Mammalian Protein-Tyrosine Phosphatase, PTP1. *J. Biol. Chem.* **1995**, *270*, 11199−11204.
(63) Chen, L.; Montserat, J.; Lawrence, D. S.; Zhang, Z. Y. VHR and PTP1 Protein Phosphatases Exhibit Remarkably Different Active Site Specificities toward Low Molecular Weight Nonpeptidic Substrates. *Biochemistry* **1996**, *35*, 9349−9354.
(64) Cleland, W. W. The Kinetics of Enzyme-Catalyzed Reactions with Two or More Substrates or Products. *Biochim. Biophys. Acta* **1963**, *67*, 104−137.

JM990329Z